Electronic Supplementary Information

Molecular balloon, Pd_6L_8 cages: Recognition of alkyl sulfate surfactants

Haeri Lee, Dongwon Kim, Hyejin Oh, and Ok-Sang Jung*

Department of Chemistry, Pusan National University, Busan 46241, Korea.

Table of Contents

Experimental Procedures

1.1. Materials and Measurements

All chemicals including $Pd(NO_3)_2$ and $AgBF_4$ were purchased from Sigma Aldrich, and used without further purification. Elemental analyses (C, H, N) were performed on crystalline samples by the KBSI Pusan Center using a Vario-EL III analyzer. Thermal analyses were performed under N_2 at a scan rate of 10 °C/min using a Labsys TGA-DSC 1600. Infrared spectra (4000–400 cm^{-1}) were obtained on a Nicolet 380 FT-IR spectrophotometer using samples prepared as KBr pellets. ^1H (500 MHz), ^1H-^1H COSY, DOSY, ^{13}C (125 MHz) NMR spectra were recorded on an AVANCE NEO 500. ^1H (600 MHz) and ^{13}C (150 MHz) spectra NMR for L were recorded on a 600 MHz Agilent NMR system in Central Laboratory at Pusan National University. Electrospray time of flight ionization mass spectrometry (ESI-TOF-MS) was recorded on a Synapt G2 mass spectrometer (WATERS) at Ochang center, KBSI. Samples were injected as a mixed dimethyl sulfoxide (Me_2SO) and acetonitrile solution (*v/v* = 1 : 250). Static contact angle of a pure water droplet was measured by Phoenix 300 apparatus (Surface & Electro-Optics Co., South Korea) equipped with a video camera. SEM images were collected by the KBSI Pusan Center using high resolution scanning electron microscope (Electron Gun; ZrO/W Shottly Gun).

1.2. Synthesis of 1,3,5-tris(4-nicotinamidephenoxy)benzene (L)

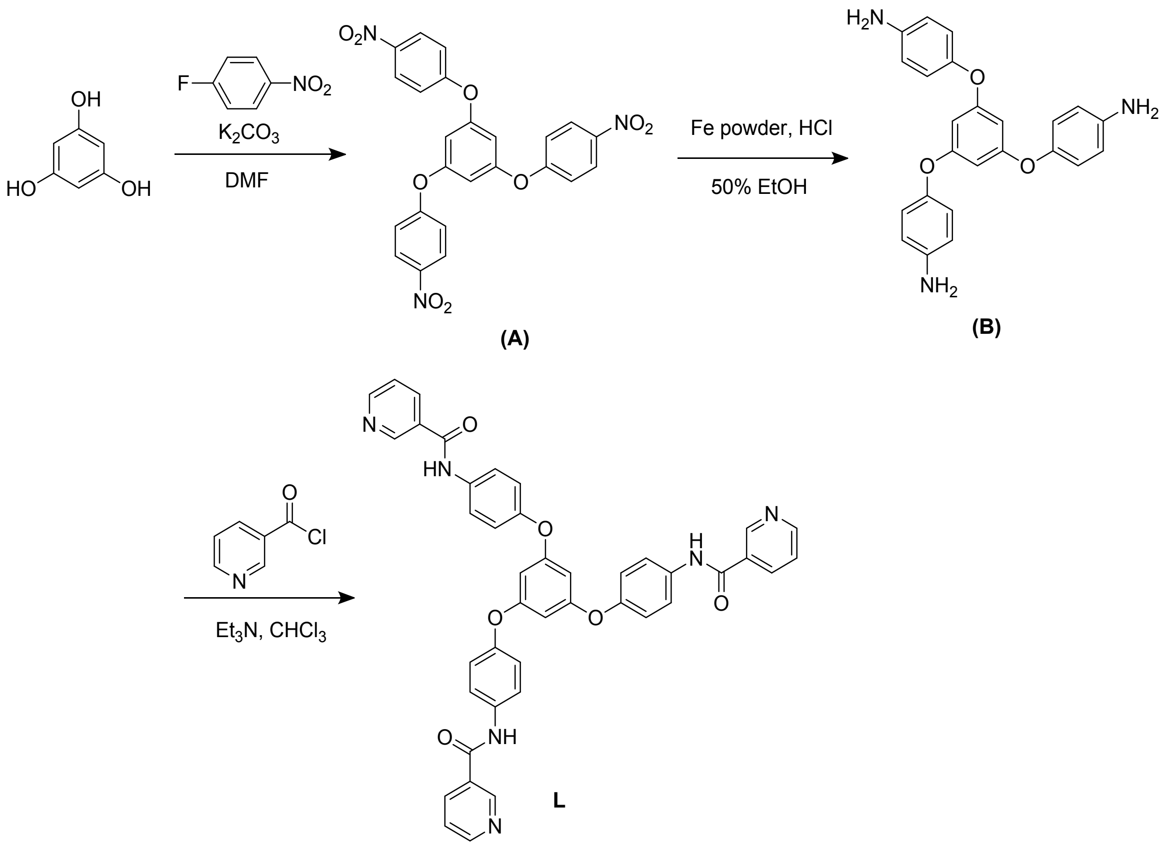

Scheme S1. Synthetic Procedure for L

A mixture of phloroglucinol (1.2 g, 10 mmol), 1-fluoro-4-nitrobenzene (4.65 g, 33 mmol), and potassium carbonate (13.5 g, 90 mmol) in 100 mL of *N,N*-dimethylformamide (DMF) was heated to 120 °C for 1 d. The reaction mixture was then cooled to room temperature and the precipitate was filtered off. 1,3,5-tris(4'-nitrophenoxy)benzene (**A**) was recrystallized in DMF/H_2O (88% yield (4.3 g)). HCl (0.6 mL concd. HCl in 10 mL of 50%

ethanol) was slowly added to a stirred solution of **A** (3.4 g, 7 mmol) and Fe powder (5.6 g, 100 mmol) in 50% ethanol (150 mL), and then stirred at 85°C for 1 d. After the reaction, 15% KOH was added and stirred for 30 min. After the precipitate was filtered off, the solution was concentrated to 30 mL under vacuo and extracted with water and chloroform. The organic layer was dried over $MgSO_4$. After removal of solvent, the residue was dried over under vacuo at 40 °C, which is produced 1,3,5-tris(4'-aminophenoxy)benzene (**B**, 2.24 g, 80%). Triethylamine (5.0 mL, 36 mmol) was slowly added into a stirred mixture of **B** (2.0 g, 5 mmol) and nicotinoyl chloride hydrochloride (3.2 g, 16.5 mmol) in chloroform (100 mL) at 65 °C, and then the reaction mixture was refluxed for 12 h. The solution was washed with water several times and then dried with $MgSO_4$. Removal of the solvent afforded a pale yellow solid of 1,3,5-tris(4-nicotinamidephenoxy)benzene in a 72% yield (2.5 g). m.p. 245°C. Anal. Calc. for $C_{42}H_{30}N_6O_6$: C, 70.58; H, 4.23; N, 11.76%. Found: C, 70.20; H, 4.12; N, 11.60%.

^{1}H NMR (600 MHz, Me_2SO-d_6, 25°C): $\delta = 10.49$ (s, 3H), 9.11 (s, 3H), 8.75 (d, ^3J(H,H) = 4.60 Hz, 3H), 8.28 (d, ^3J(H,H) = 7.89 Hz, 3H), 7.82 (d, ^3J(H,H) = 8.55 Hz, 6H), 7.54 (dd, ^3J(H,H) = 7.89 Hz, ^3J(H,H) = 4.60 Hz, 3H), 7.13 (d, ^3J(H,H) = 8.55 Hz, 6H), 6.31 (s, 3H).

^{13}C NMR (150 MHz, Me_2SO-d_6, 25°C): $\delta = 163.94$, 159.69, 152.09, 151.27, 148.68, 135.43, 135.33, 130.52, 123.46, 122.05, 119.89, 101.51.

IR (KBr): cm^{-1}=3519 (w), 3245 (w), 3188 (w), 3122 (w), 3054 (w), 1656 (m, −CONH−), 1614 (m), 1594 (m), 1548 (m), 1504 (s), 1456 (m), 1410 (m), 1322 (m), 1272 (w), 1214 (s), 1168 (w), 1118 (m), 1006 (m), 827 (w), 732 (w), 707 (w).

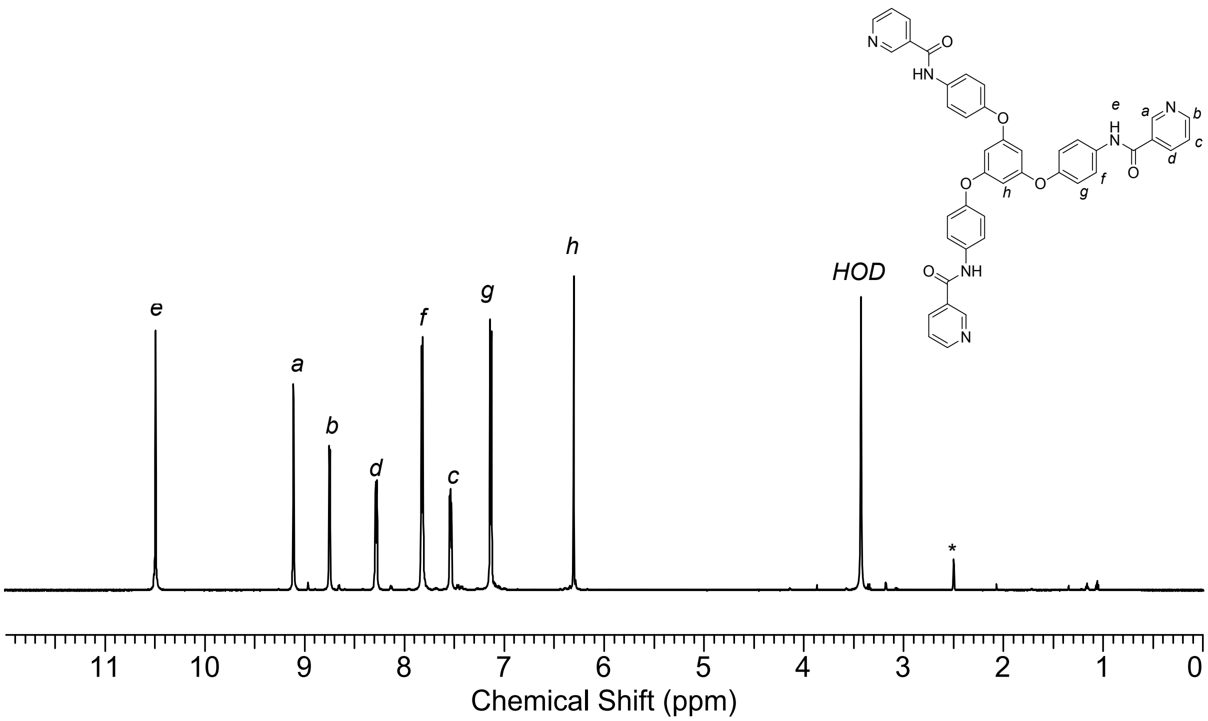

Fig. S1. ^{1}H NMR spectrum for L in Me$_2$SO-d_6.

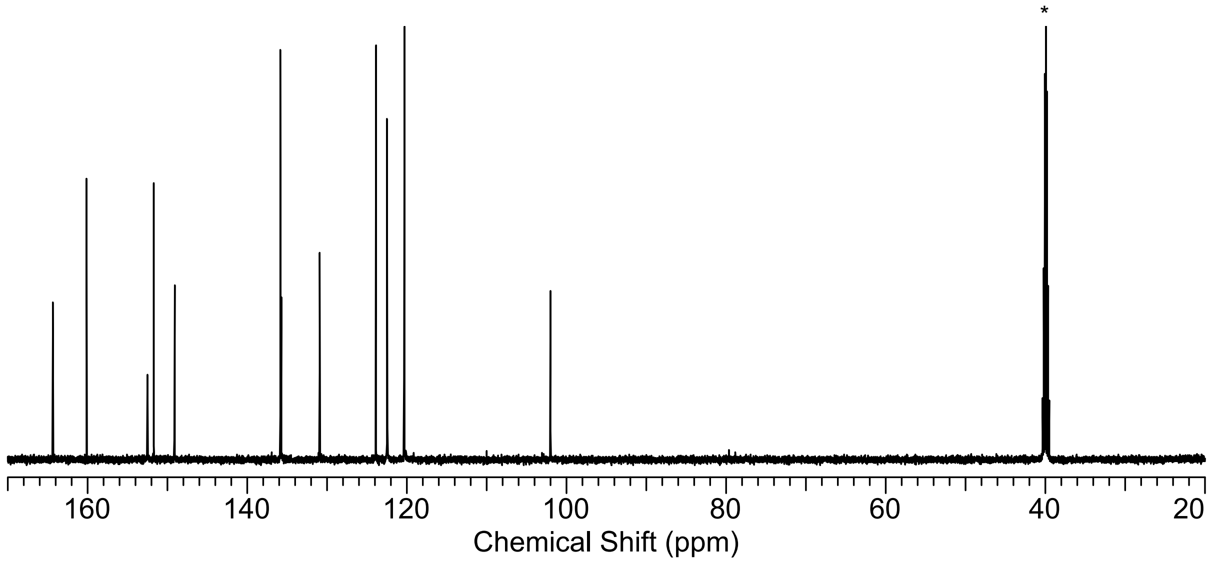

Fig. S2. ^{13}C NMR spectrum for L in Me$_2$SO-d_6.

1.3. Synthesis of $[Pd_6L_8](NO_3)_{12}\cdot 40(Me_2SO)\cdot 9$(Ethyl acetate)$\cdot 3$(Toluene) ($1\cdot 12NO_3$)

A Me_2SO solution (5.0 mL) of L (0.24 mmol, 171 mg) was slowly added to a Me_2SO solution (5.0 mL) of $Pd(NO_3)_2$ (0.18 mmol, 41.4 mg) at 70°C. After vigorous stirring at the same temperature for 5 h, toluene and ethyl acetate (*v/v* = 1 : 2) were slowly diffused into the resulting solution. Colorless crystals suitable for X-ray crystallography were obtained in a week (65 % yield on metal basis, 138 mg). m.p. 367°C (dec.) Anal. Calc. for $C_{336}H_{240}N_{60}O_{84}Pd_6\cdot 25C_2H_6SO$: C, 51.21; H, 4.34; N, 9.28%. Found: C, 50.90; H, 4.29; N, 9.38%.

^{1}H NMR (600 MHz, Me_2SO-d_6, 25°C): δ = 10.59 (s, 24H), 10.15 (s, 24H), 9.52 (br, 24H), 8.70 (d, ^3J(H,H) = 7.04 Hz, 24H), 7.94 (d, ^3J(H,H)=8.22 Hz, 48H), 7.92 (m, 24H), 7.19 (d, ^3J(H,H) = 8.22 Hz, 48H), 5.96 (s, 24H).

^{13}C NMR (150 MHz, Me_2SO-d_6, 25°C): δ = 161.50, 161.06, 153.53, 152.53, 150.43, 139.75, 138.95, 136.48, 127.15, 122.34, 122.08, 97.69.

IR (KBr): cm^{-1} = 3266 (br), 3199 (br), 3072 (w), 1675 (m), 1610 (m), 1594 (m), 1504 (s), 1482 (m), 1410 (m), 1382 (w, NO_3^-), 1319 (m), 1270 (w), 1209 (s), 1168 (w), 1116 (m), 1002 (m), 829 (m), 694 (m).

ESI-TOF-HR-MS: *m/z* =1711.2797 (calc. for $[Pd_6L_8(NO_3)_{12} - 4NO_3^-]^{4+}$ 1711.276), 1397.6473 (calc. for $[Pd_6L_8(NO_3)_{12} - 5NO_3^-]^{5+}$, 1391.661).

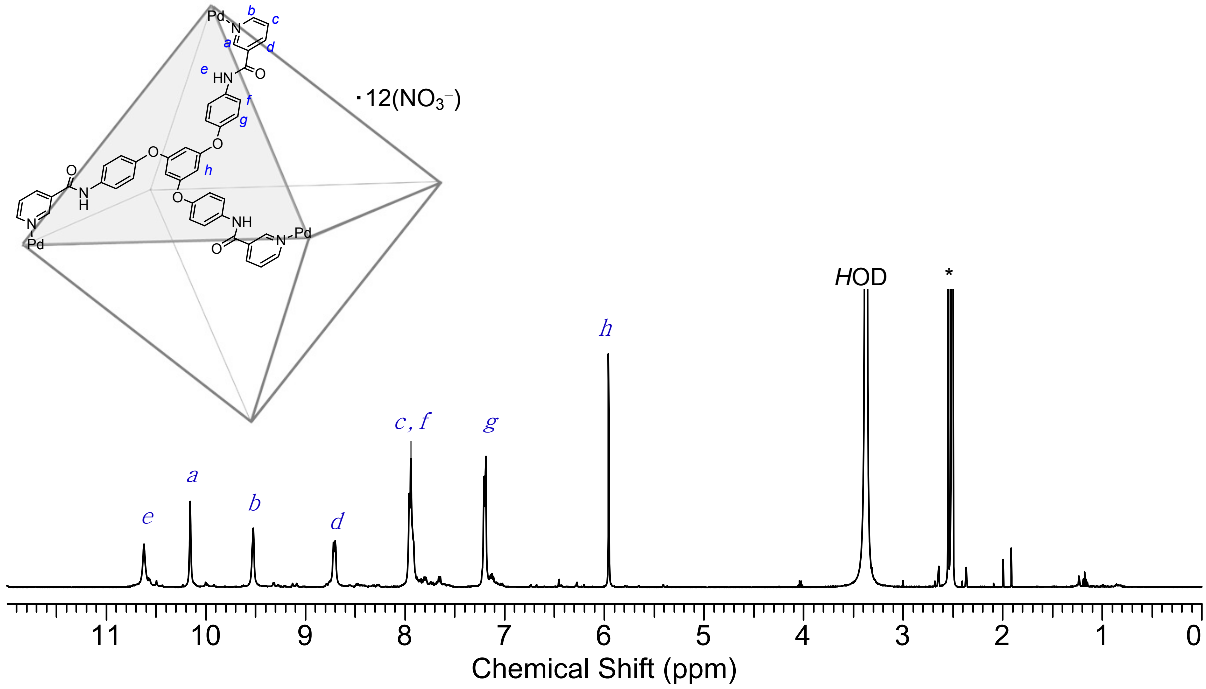

Fig. S3. ^{1}H NMR spectrum (in Me$_2$SO-d_6) for the crystals of **1**·12NO$_3$ (*: the residue of Me$_2$SO).

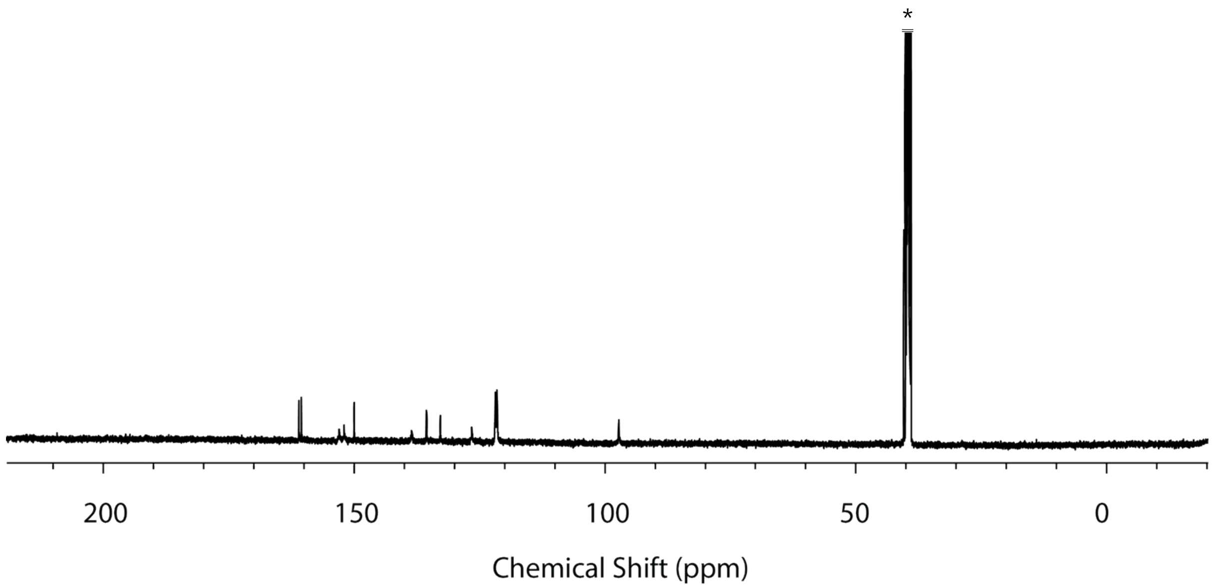

Fig. S4. ^{13}C NMR spectrum (in Me_2SO-d_6) for the crystals of **1**·12NO_3 (*: the residue of Me_2SO).

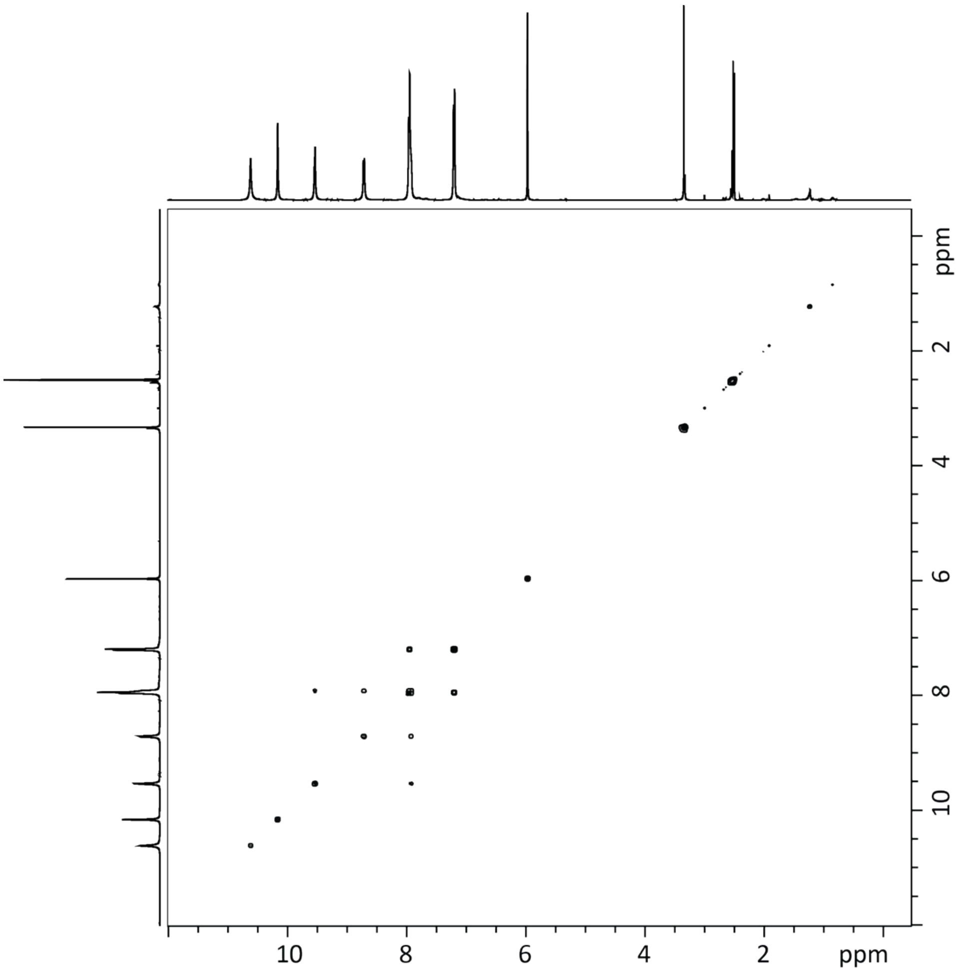

Fig. S5. ^1H-^1H COSY spectra for the crystals of **1**·12NO$_3$ in Me$_2$SO-d_6 (^1H NMR assignments are represented in Fig. S3).

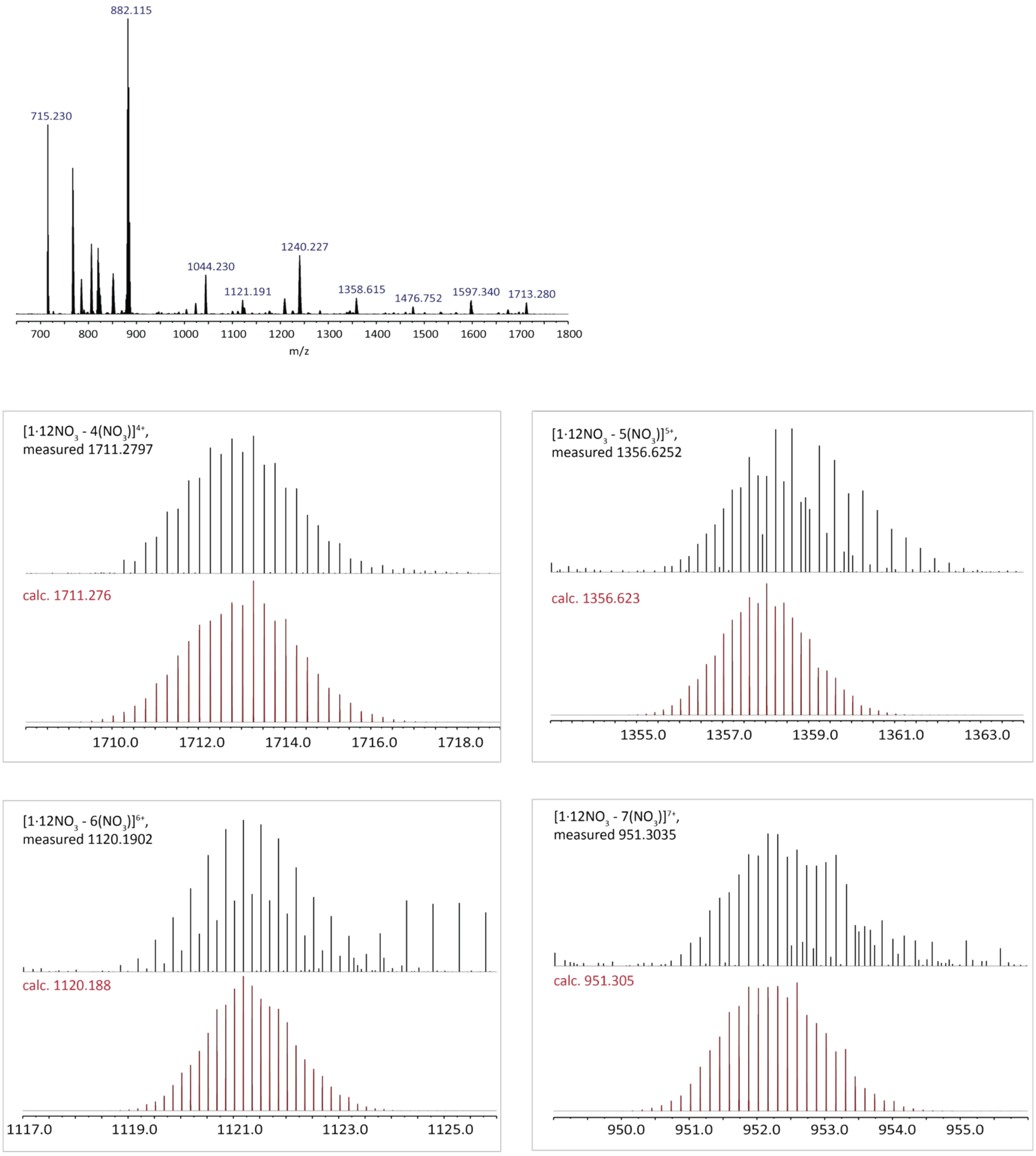

Fig. S6. HR-ESI-TOF-MS spectra for **1**·12NO$_3$, other fragment was assigned as [L + H$^+$]$^+$ = 715.2298 (calc. 715.230), [Pd^{2+}L(NO$_3^-$)]$^+$ = 882.1143 (calc. 882.113).

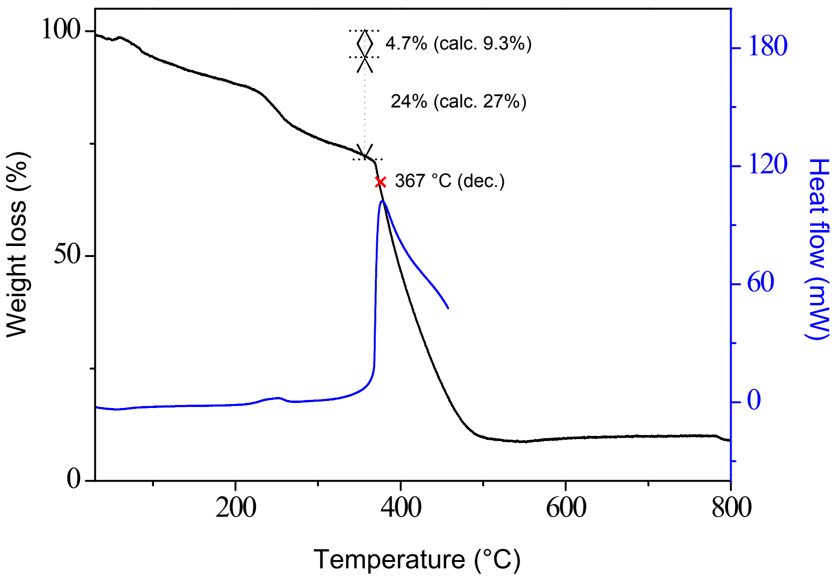

Fig. S7. TG analysis and DSC curves for crystals of **1**·12NO$_3$.

1.4. Synthesis of $[Pd_6L_8](BF_4)_{12}\cdot 35(Me_2SO)\cdot 12(THF)$ ($1\cdot 12BF_4$)

An acetonitrile solution of $AgBF_4$ (0.48 mmol, 93 mg) was added to an acetonitrile solution of $PdCl_2(CH_3CN)_2$ (0.24 mmol, 63 mg) at 70°C. The reaction solution was stirred for 1 h at the same temperature. After cooling and the filtration of AgCl, acetonitrile was fully evaporated by rotary evaporator. A Me_2SO solution (5 mL) of L (0.24 mmol, 171 mg) was added a Me_2SO solution (5 mL) of $[Pd(CH_3CN)_4](BF_4)_2$ (0.18 mmol, 80 mg). After vigorous stirring maintaining at 70°C for 5 h, tetrahydrofuran was slowly diffused into the resulting solution. Colorless crystals suitable for X-ray crystallography were obtained in a week (72 % yield on metal basis, 159 mg). m.p. 297°C (dec.) Anal. Calc. for $C_{336}H_{240}N_{48}O_{48}B_{12}F_{48}Pd_6\cdot 20C_2H_6SO$: C, 50.40; H, 4.05; N, 7.50%. Found: C, 50.17; H, 3.96; N, 8.00%.

^{1}H NMR (600 MHz, Me_2SO-d_6, 25°C): $\delta = 10.59$ (s, 24H), 10.15 (s, 24H), 9.50 (br, 24H), 8.71 (d, ^3J(H,H) = 7.63 Hz, 24H), 7.94 (d, ^3J(H,H) = 8.80 Hz, 48H), 7.92 (m, 24H), 7.19 (d, ^3J(H,H) = 8.80 Hz, 48H), 5.96 (s, 24H).

^{13}C NMR (125 MHz, Me_2SO-d_6, 25°C): $\delta = 161.07$, 160.59, 153.03, 152.05, 150.01, 138.58, 135.64, 132.83, 126.63, 121.88, 121.64, 97.18.

IR (KBr): $cm^{-1} = 3379$ (br), 3059 (br), 3072 (w), 1674 (m), 1610 (m), 1597 (m), 1547 (s), 1504 (s), 1454 (m), 1434 (w), 1407 (m), 1317 (m), 1211 (s), 1168 (w), 1122 (m), 1084 (m), 1038 (br, BF_4^-), 1016 (s), 950 (m), 829 (m), 694 (m).

ESI-TOF-HR-MS: $m/z = 1391.6494$ (calc. for $[Pd_6L_8(BF_4)_{12} - 5BF_4^-]^{5+}$, 1391.644), 1145.2067 (calc. for $[Pd_6L_8(BF_4)_{12} - 6BF_4^-]^{6+}$, 1145.2027).

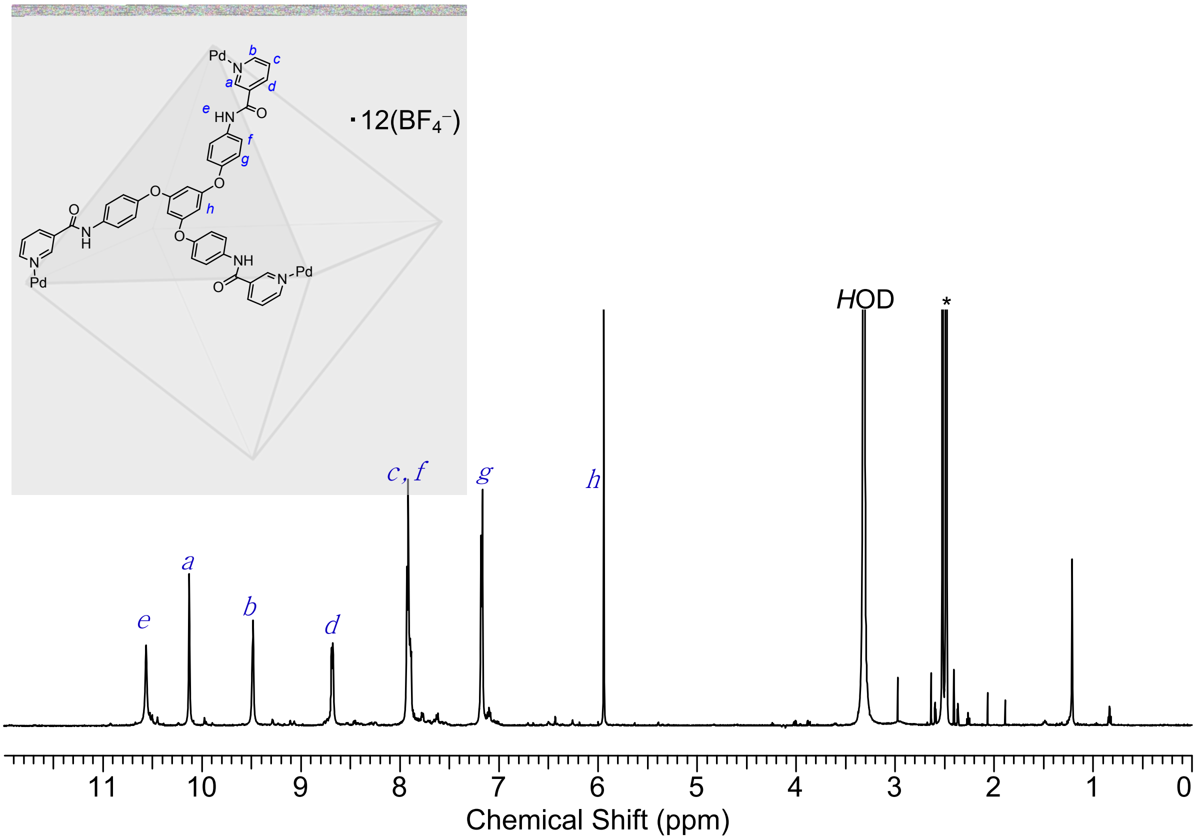

Fig. S8. ^{1}H NMR spectrum (in Me$_2$SO-d_6) for the crystals of **1**·12BF$_4$ (*: the residue of Me$_2$SO).

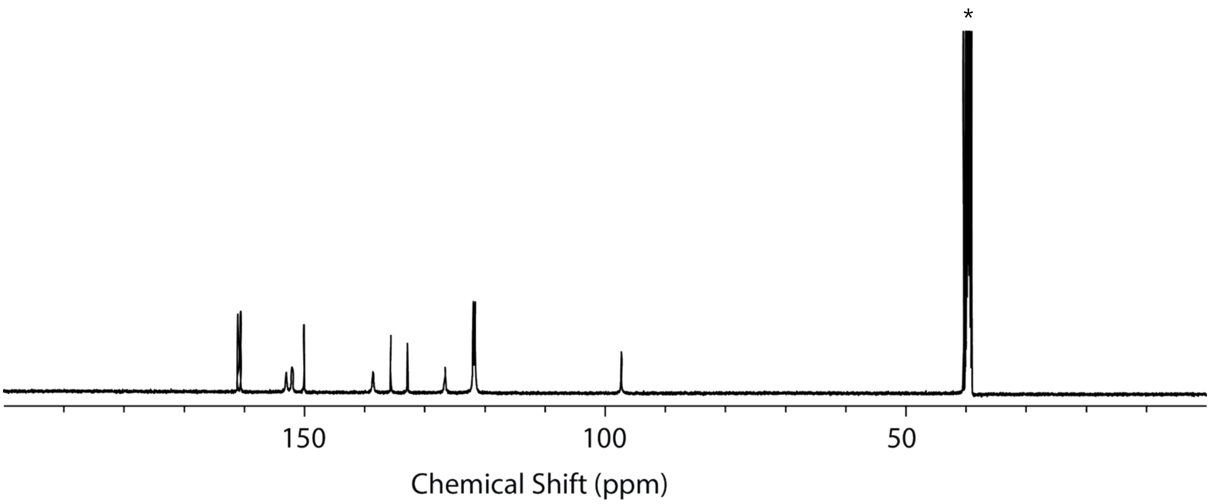

Fig. S9. ^{13}C NMR spectrum (in Me_2SO-d_6) for the crystals of **1**·$12BF_4$ (*: the residue of Me_2SO).

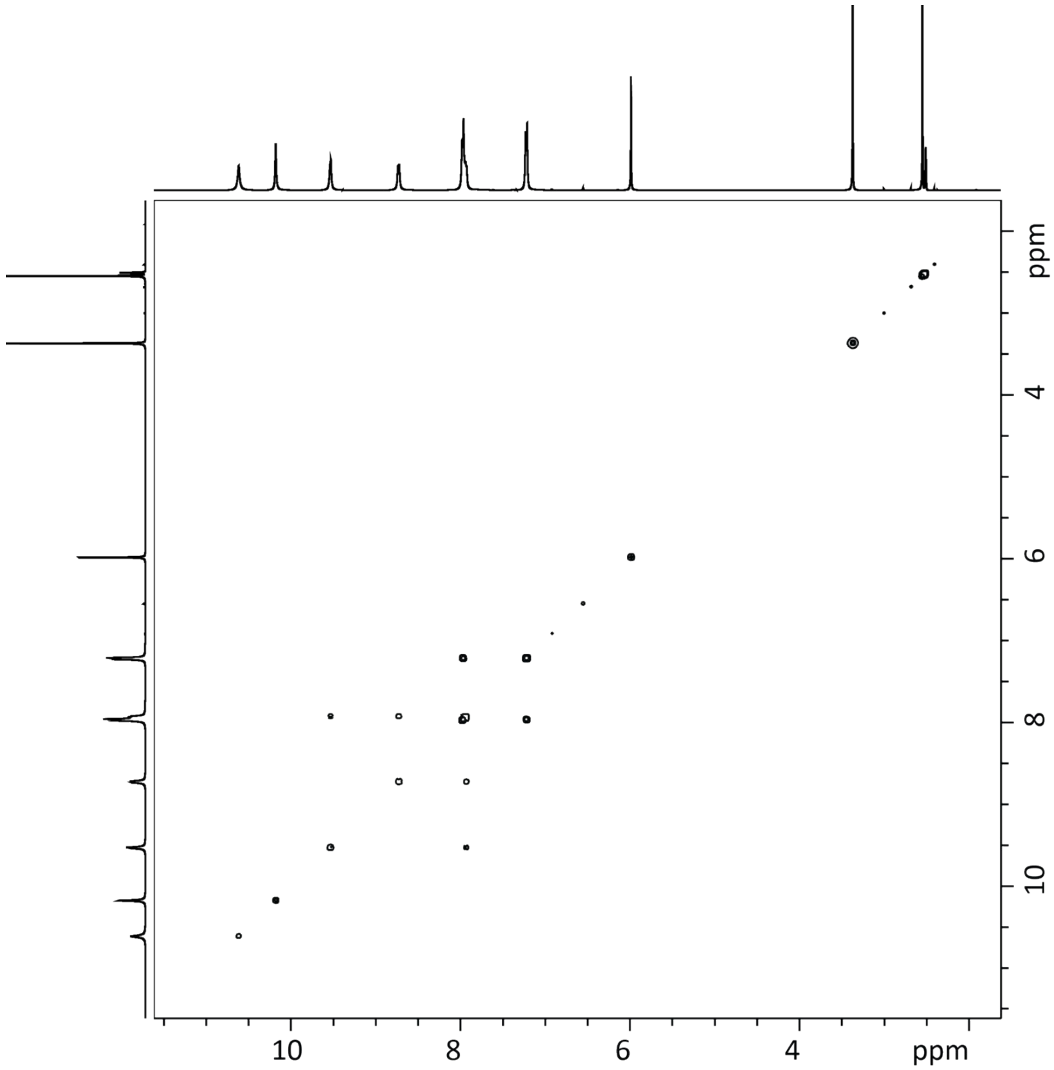

Fig. S10. ^1H-^1H COSY spectra for the crystals of **1**·12BF$_4$ in Me$_2$SO-d_6 (^1H NMR assignments are represented in Fig. S8).

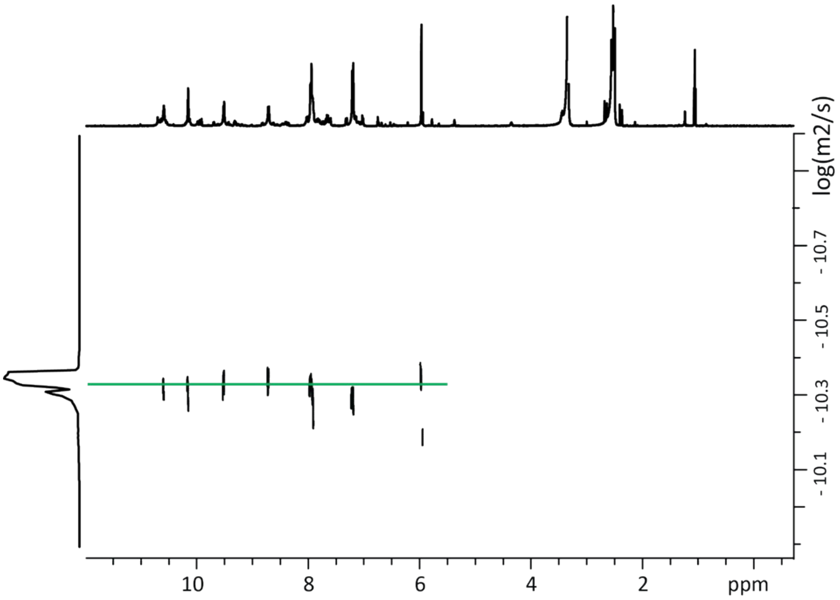

Fig. S11. DOSY spectrum for the crystals of **1**·12BF$_4$ in Me$_2$SO-d_6 at 298 K (D = 5.20 x 10^{-11}, logD = −10.284).

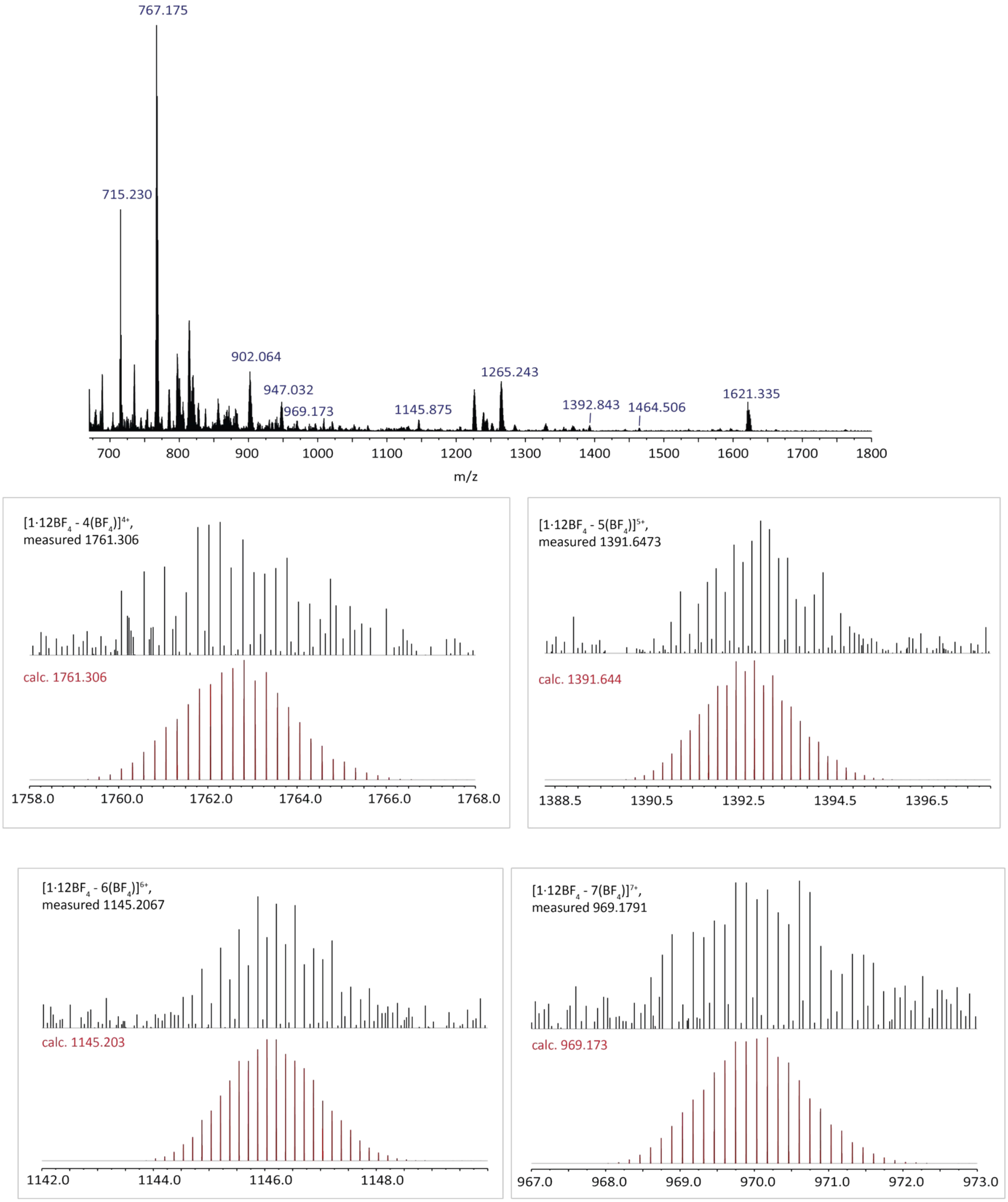

Fig. S12. HR-ESI-TOF-MS spectra for **1**·12BF$_4$, other fragment was assigned as $[L + H^+]^+$ = 715.2295 (calc. 715.230), $[Pd^{2+}L_2]^{2+}$ = 767.1752 (calc. 767.174).

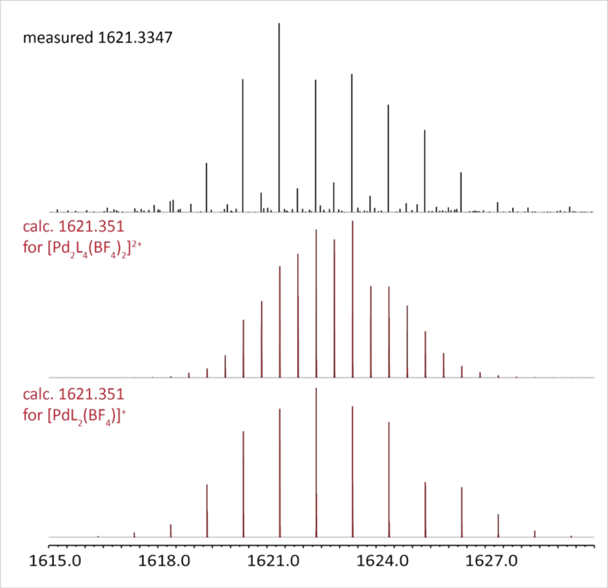

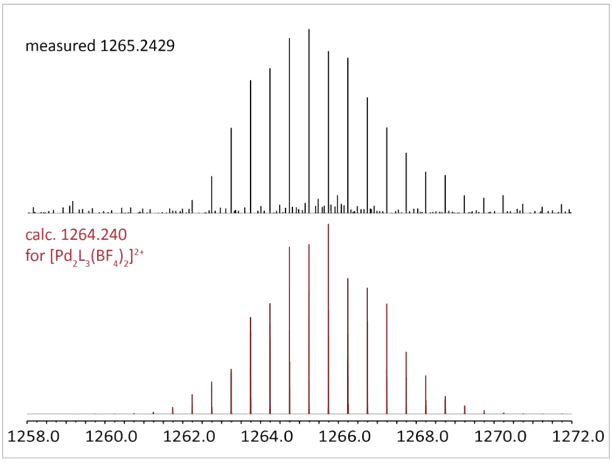

Fig. S13. *m/z* assignment for the fragment in HR-ESI-TOF-MS spectra.

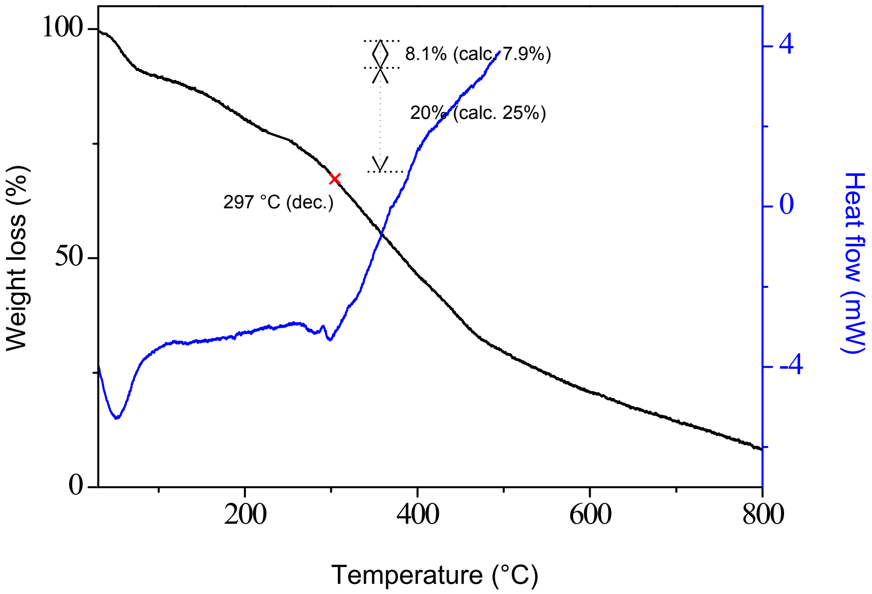

Fig. S14. TG analysis and DSC curves for crystals of **1**·12BF$_4$.

1.5. Synthesis of $[Pd_6L_8](C_nH_{2n+1}OSO_3)_{12}$ ($\mathbf{2}\cdot12C_nH_{2n+1}OSO_3$) ($n$ = 2, 8, 10, 12, 14)

Crystallization by the direct method: A Me_2SO solution of tetrabutylammonium ethyl-, octyl-, decyl-, dodecyl-, or tetradecyl sulfate (0.24 mmol) was added to the mixed solution of L (0.24 mmol, 171 mg) and $[Pd(CH_3CN)_4](BF_4)_2$ (0.18 mmol, 65 mg) in Me_2SO. Then the reaction solution was vigorous stirring at 70°C for 5 h. THF was slowly added into the resulting solution. After 10-14 days, crystalline solid of $\mathbf{2}\cdot12C_nH_{2n+1}OSO_3$ were obtained.

Anion exchange process: $\mathbf{1}\cdot12NO_3$ (or $\mathbf{1}\cdot12BF_4$) an acetone solution of $C_{12}H_{25}OSO_3^{-}NBu_4^{+}$ (30 equiv.) added slowly into dispersion sample of $\mathbf{1}\cdot12NO_3$ an aqueous solution at room temperature. After 2 h vigorous stirring at the same temperature, crystalline solid was filtered and dried over P_2O_5 for 5 h.

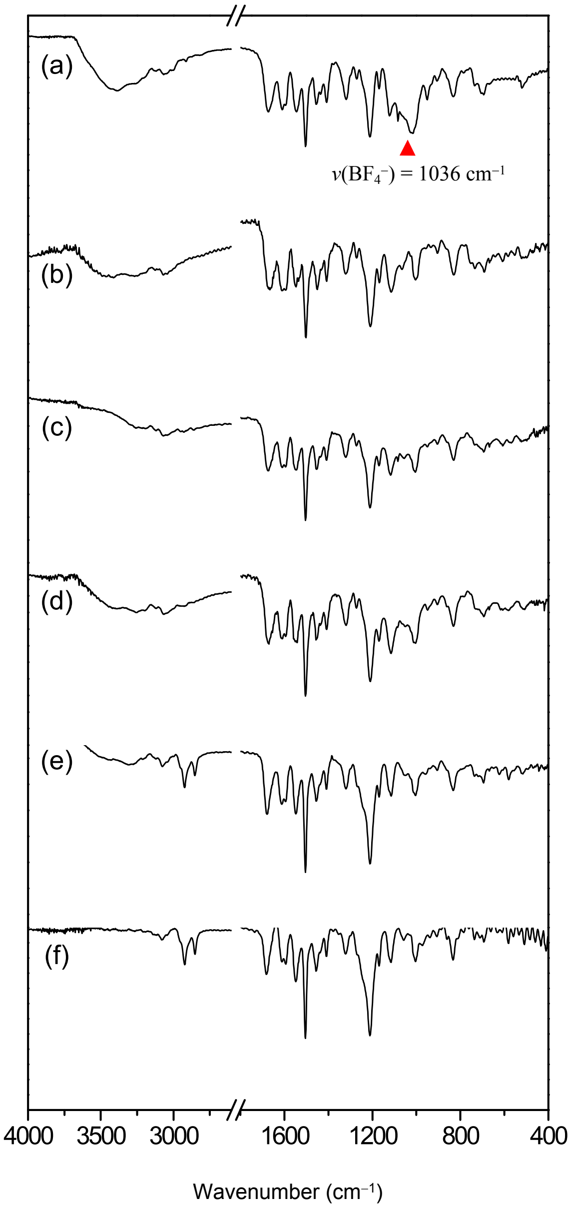

Fig. S15. IR spectra for **1**·12BF$_4$ (a), **2**·12C$_2$H$_5$OSO$_3$ (b), **2**·12C$_8$H$_{17}$OSO$_3$ (c), **2**·12C$_{10}$H$_{21}$OSO$_3$ (d), **2**·12C$_{12}$H$_{25}$OSO$_3$ (e), and **2**·12C$_{14}$H$_{29}$OSO$_3$ (f).

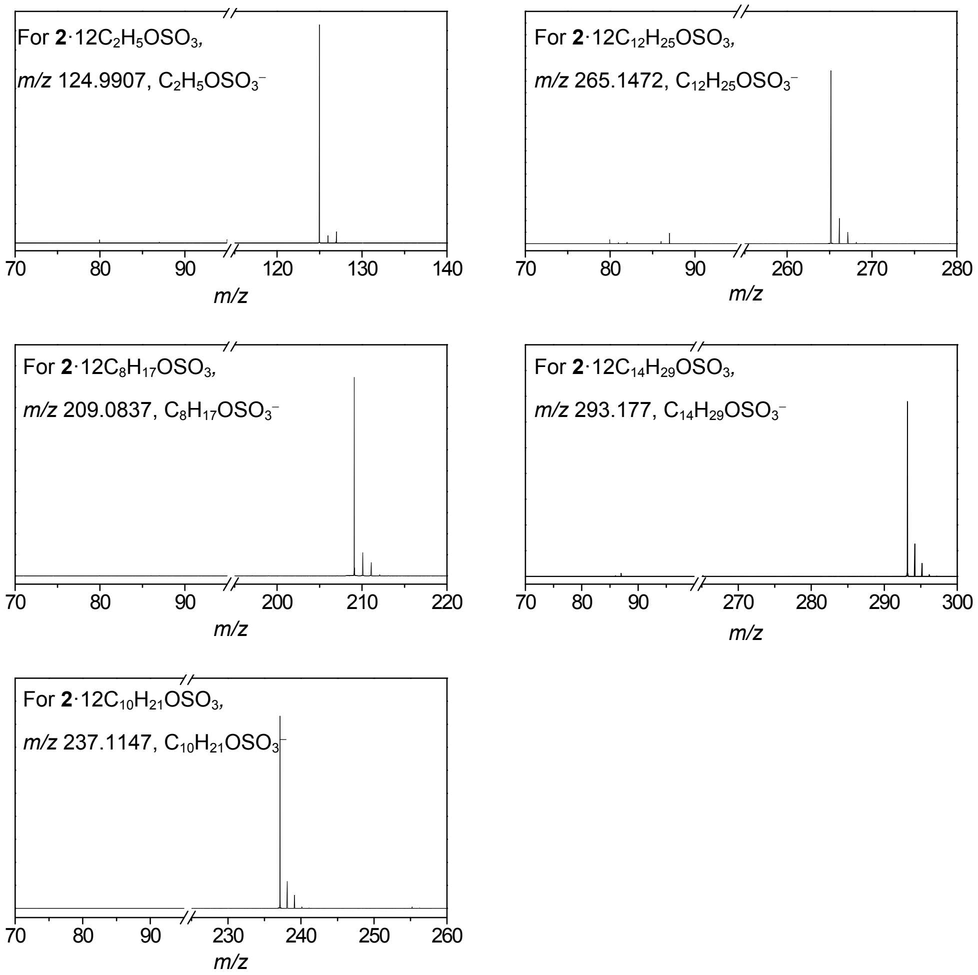

Fig. S16. Negative mode HR-ESI-TOF-Mass spectra for cage **2**.

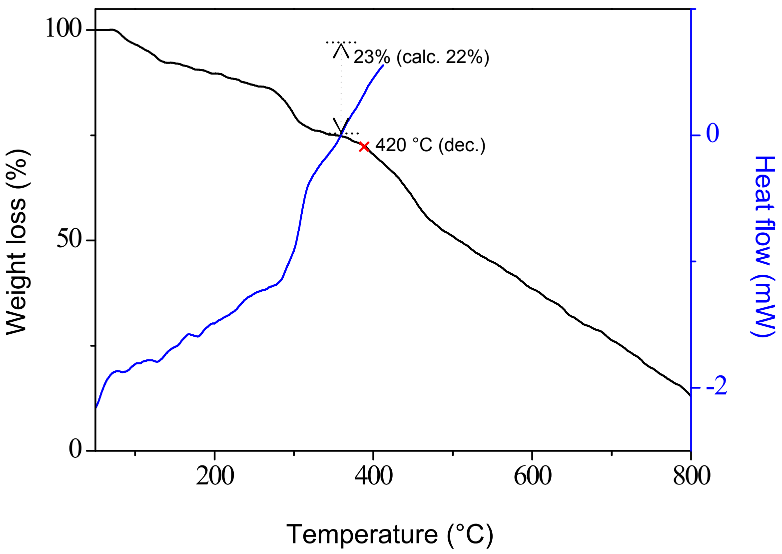

Fig. S17. TG analysis and DSC curves for **2**·$12C_{12}H_{25}OSO_3$.

2. Crystal Structure Determination

Crystals for **1**·$12NO_3$, **2**·$12C_8H_{17}OSO_3$, and **2**·$12C_{12}H_{25}OSO_3$ were directly coated with paratone-N oil and mounted with a cryoloop attached to goniohead, and transferred to a cold stream of liquid nitrogen (100K). Since **1**·$12BF_4$ was highly volatile, the crystal was sealed in 0.3 mm capillary with small amount of mother liquor and data collection carried out at 298K. The diffraction data measured using synchrotron X-ray (λ = 0.80000 Å for **1**·$12NO_3$, 0.90000 Å for **2**·$12C_8H_{17}OSO_3$, and 0.75000 Å for **1**·$12BF_4$ and **2**·$12C_{12}H_{25}OSO_3$) ADSC Quantum 210 CCD detector with a silicon (111) double-crystal monochromator at BL2D SMC beamline of the Pohang Accelerator Laboratory, South Korea. The PAL BL2D-SMDC program[1] was used for data collection (detector distance is 62 mm, omega scan; $\Delta\omega = 1°$, exposure time is 20 sec per frame) and HKL3000sm (Ver. 715)[2] was used for cell refinement, reduction, and absorption correction.

2.1. Refinement Details

The crystal structures were solved by the direct method with SHELXT-2014 program[3] and refined by full-matrix least-squares calculations with the SHELXL-2014/7 program package.[4] Detailed crystallographic data were shown in Table S1. For **1**·$12NO_3$, **1**·$12BF_4$, **2**·$12C_8H_{17}OSO_3$, and **2**·$12C_{12}H_{25}OSO_3$, anions and solvate molecules in the voids were highly disordered in a large volume. The residual electron density was treated as a diffuse contribution using the SQUEEZE in the PLATON software in order to locate a series of voids.[5] Techniques commonly applied for macromolecular structures were employed to generate a molecular model and increase robustness of the refinement. L (NPB), octyl sulfate (SO8), and dodecyl sulfate (DSO) structures were generated by the GRADE program using the GRADE Web Server (http://grade.globalphasing.org) and applied in the refinement. A GRADE dictionary for SHELXL contains target values and standard deviations for 1.2-distances (DFIX) and 1.3-distances (DANG), as well as restraints for planar groups (FLAT). The refinement of ADP's for non-hydrogen atoms was enabled by using the rigid bond restraint (RIGU)[6] in the SHELXL program. SIMU restraints were additionally employed The TABS keyword behind the ACTA instruction was employed to generate the CIF.

Table S1. Crystal Data and Refinement Parameters for **1**·12NO$_3$, **1**·12BF$_4$, **2**·12C$_8$H$_{17}$OSO$_3$, and **2**·12C$_{12}$H$_{25}$OSO$_3$

	1·12NO$_3$	**1**·12BF$_4$	**2**·12C$_8$H$_{17}$OSO$_3$	**2**·12C$_{12}$H$_{25}$OSO$_3$
CCDC number	1888048	1888049	1888050	1888051
Empirical formula	$C_{360}H_{312}N_{58}O_{90}Pd_6S_{12}$	$C_{336}H_{240}N_{48}O_{48}Pd_6$	$C_{396}H_{378}N_{48}O_{78}Pd_6S_{12}$	$C_{420}H_{426}N_{48}O_{78}Pd_6S_{12}$
Formula weight	7913.78	6356.15	8080.56	8417.18
Temperature	103(2) K	298(2) K	100(2) K	103(2) K
Wavelength	0.800 Å	0.750 Å	0.900 Å	0.750 Å
Crystal system	Triclinic	Tetragonal	Trigonal	Trigonal
Space group	*P*-1	*I*4/*m*	*R*-3	*R*-3
a (Å)	a = 26.739(5)	a = 35.325(5)	a = 29.802(4)	a = 29.879(4)
b (Å)	b = 26.793(5)	b = 35.325(5)	b = 29.802(4)	b = 29.879(4)
c (Å)	c = 29.537(6)	c = 49.962(10)	c = 68.496(14)	c = 68.309(14)
α (°)	a= 64.09(3)	a= 90	a= 90	a= 90
β (°)	b= 77.30(3)	b= 90	b= 90	b= 90
γ (°)	g = 86.34(3)	g = 90	g = 120	g = 120
V (Å^3)	18556(8)	62345(22)	52684(18)	52813(18)
Z	1	2	3	3
Density (calculated)	0.708 Mg/m^3	0.339 Mg/m^3	0.764 Mg/m^3	0.794 Mg/m^3
Absorption coefficient	0.298 mm^{-1}	0.119 mm^{-1}	0.431 mm^{-1}	0.266 mm^{-1}
F(000)	4066	6504	12546	13122
Crystal size	0.300 x 0.255 x 0.252 mm^3	0.200 x 0.200 x 0.200 mm^3	0.141 x 0.098 x 0.091 mm^3	0.120 x 0.030 x 0.030 mm^3
Theta range for data collection	1.272 to 26.150°.	0.745 to 30.733°.	1.068 to 20.243°.	1.042 to 24.500°.
Index ranges	-29<=h<=29, -29<=k<=29, -32<=l<=32	-47<=h<=47, -41<=k<=41, -64<=l<=63	-22<=h<=19, -22<=k<=22, -52<=l<=29	-33<=h<=33, -33<=k<=33, -75<=l<=75
Reflections collected	94599	178025	15908	82624
Independent reflections	48002 [R(int) = 0.0354]	36294 [R(int) = 0.1236]	5568 [R(int) = 0.0988]	16590 [R(int) = 0.1293]
Completeness to theta = 26.150°	92.30%	99.90%	99.80%	99.70%
Absorption correction	Empirical	Empirical	Empirical	Empirical
Max. and min. transmission	1.000 and 0.911	0.977 and 0.977	0.962 and 0.942	0.992 and 0.969
Refinement method	Full-matrix least-squares on F^2	Full-matrix least-squares on F^2	Full-matrix least-squares on F^2	Full-matrix least-squares on F^2
Data / restraints / parameters	48002 / 3267 / 2370	36294 / 988 / 497	5568 / 1527 / 821	16590 / 1555 / 848
Goodness-of-fit on F2	1.341	0.955	1.852	1.122
Final R indices [I>2sigma(I)]	$R_1 = 0.1122$, $wR_2 = 0.3608$	$R_1 = 0.1517$, $wR_2 = 0.3986$	$R_1 = 0.1499$, $wR_2 = 0.4205$	$R_1 = 0.1295$, $wR_2 = 0.3671$
R indices (all data)	$R_1 = 0.1503$, $wR_2 = 0.3831$	$R_1 = 0.3047$, $wR_2 = 0.4698$	$R_1 = 0.2036$, $wR_2 = 0.4504$	$R_1 = 0.2257$, $wR_2 = 0.4149$
Largest diff. peak and hole	0.953 and -0.937 e.Å^{-3}	1.067 and -0.578 e.Å^{-3}	1.112 and -0.701 e.Å^{-3}	0.822 and -0.658 e.Å^{-3}
Radiation	Synchrotron	Synchrotron	Synchrotron	Synchrotron

$^aR_1 = \Sigma||F_o|-|F_c||/\Sigma|F_o|$, $^bwR_2 = (\Sigma w(F_o^2-F_c^2)^2/\Sigma w(F_o^2)^2)^{1/2}$

Table S2. Selected bond lengths (Å) and angles (°) **1**·12NO$_3$, **1**·12BF$_4$, **2**·12C$_8$H$_{17}$OSO$_3$, and **2**·12C$_{12}$H$_{25}$OSO$_3$

1·12NO$_3$		**1**·12BF$_4$		**2**·12C$_8$H$_{17}$OSO$_3$		**2**·12C$_{12}$H$_{25}$OSO$_3$	
Pd11-N14	2.007(6)	Pd11-N53$^{\#1}$	2.002(6)	Pd11-N32$^{\#1}$	1.969(18)	Pd11-N52$^{\#1}$	1.994(8)
Pd11-N57	2.014(6)	Pd11-N53	2.002(6)	Pd11-N13	2.024(14)	Pd11-N13	2.006(9)
Pd11-N16	2.022(7)	Pd11-N13$^{\#2}$	2.048(6)	Pd11-N52$^{\#2}$	2.024(18)	Pd11-N32$^{\#2}$	2.024(8)
Pd11-N35	2.027(6)	Pd11-N13$^{\#3}$	2.048(6)	Pd11-N12	2.034(17)	Pd11-N12	2.024(9)
Pd22-N15$^{\#1}$	2.000(7)	Pd22-N33$^{\#2}$	2.005(6)				
Pd22-N17	2.002(6)	Pd22-N33$^{\#4}$	2.005(6)				
Pd22-N36$^{\#1}$	2.006(6)	Pd22-N33$^{\#5}$	2.005(6)				
Pd22-N34	2.010(7)	Pd22-N33	2.005(6)				
Pd33-N37	2.015(7)						
Pd33-N55$^{\#1}$	2.018(8)						
Pd33-N56	2.024(7)						
Pd33-N54$^{\#1}$	2.031(6)						
N14-Pd11-N57	90.1(3)	N53$^{\#1}$-Pd11-N53	88.4(4)	N32$^{\#1}$-Pd11-N13	91.3(7)	N52$^{\#1}$-Pd11-N13	90.6(4)
N14-Pd11-N16	178.1(3)	N53$^{\#1}$-Pd11-N13$^{\#2}$	178.3(3)	N32$^{\#1}$-Pd11-N52$^{\#2}$	175.9(9)	N52$^{\#1}$-Pd11-N32$^{\#2}$	177.6(4)
N57-Pd11-N16	91.0(3)	N53-Pd11-N13$^{\#2}$	90.0(2)	N13-Pd11-N52$^{\#2}$	88.8(8)	N13-Pd11-N32$^{\#2}$	89.3(4)
N14-Pd11-N35	90.1(3)	N53$^{\#1}$-Pd11-N13$^{\#3}$	90.0(2)	N32$^{\#1}$-Pd11-N12	90.9(9)	N52$^{\#1}$-Pd11-N12	88.3(4)
N57-Pd11-N35	175.2(3)	N53-Pd11-N13$^{\#3}$	178.3(3)	N13-Pd11-N12	177.8(9)	N13-Pd11-N12	176.2(4)
N16-Pd11-N35	88.6(3)	N13$^{\#2}$-Pd11-N13$^{\#3}$	91.5(3)	N52$^{\#2}$-Pd11-N12	89.1(10)	N32$^{\#2}$-Pd11-N12	91.7(4)
N15$^{\#1}$-Pd22-N17	90.3(3)	N33$^{\#2}$-Pd22-N33$^{\#4}$	89.998(3)				
N15$^{\#1}$-Pd22-N36$^{\#1}$	91.7(3)	N33$^{\#2}$-Pd22-N33$^{\#5}$	179.3(4)				
N17-Pd22-N36$^{\#1}$	177.9(3)	N33$^{\#4}$-Pd22-N33$^{\#5}$	89.998(2)				
N15$^{\#1}$-Pd22-N34	177.8(3)	N33$^{\#2}$-Pd22-N33	90.000(3)				
N17-Pd22-N34	90.7(3)	N33$^{\#4}$-Pd22-N33	179.3(4)				
N36$^{\#1}$-Pd22-N34	87.3(3)	N33$^{\#5}$-Pd22-N33	89.997(3)				
N37-Pd33-N55$^{\#1}$	89.5(4)						
N37-Pd33-N56	90.0(4)			Pd···OSO$_3$R	3.95(2)	Pd···OSO$_3$R	4.04(1)
N55$^{\#1}$-Pd33-N56	175.8(3)				4.23(2)		3.92(1)
N37-Pd33-N54$^{\#1}$	175.5(3)				3.96(2)		4.20(1)
N55$^{\#1}$-Pd33-N54$^{\#1}$	89.7(3)						
N56-Pd33-N54$^{\#1}$	90.5(3)						
$^{\#1}$ -x+1,-y,-z+1		$^{\#1}$ x,y,-z, $^{\#2}$ y,-x+1,z $^{\#3}$ y,-x+1,-z $^{\#4}$ -x+1,-y+1,z $^{\#5}$ -y+1,x,z		$^{\#1}$ y+1/3,-x+y+2/3,-z+2/3 $^{\#2}$ x-y+1/3,x-1/3,-z+2/3		$^{\#1}$ x-y+1/3,x-1/3,-z+2/3 $^{\#2}$ y+1/3,-x+y+2/3,-z+2/3	

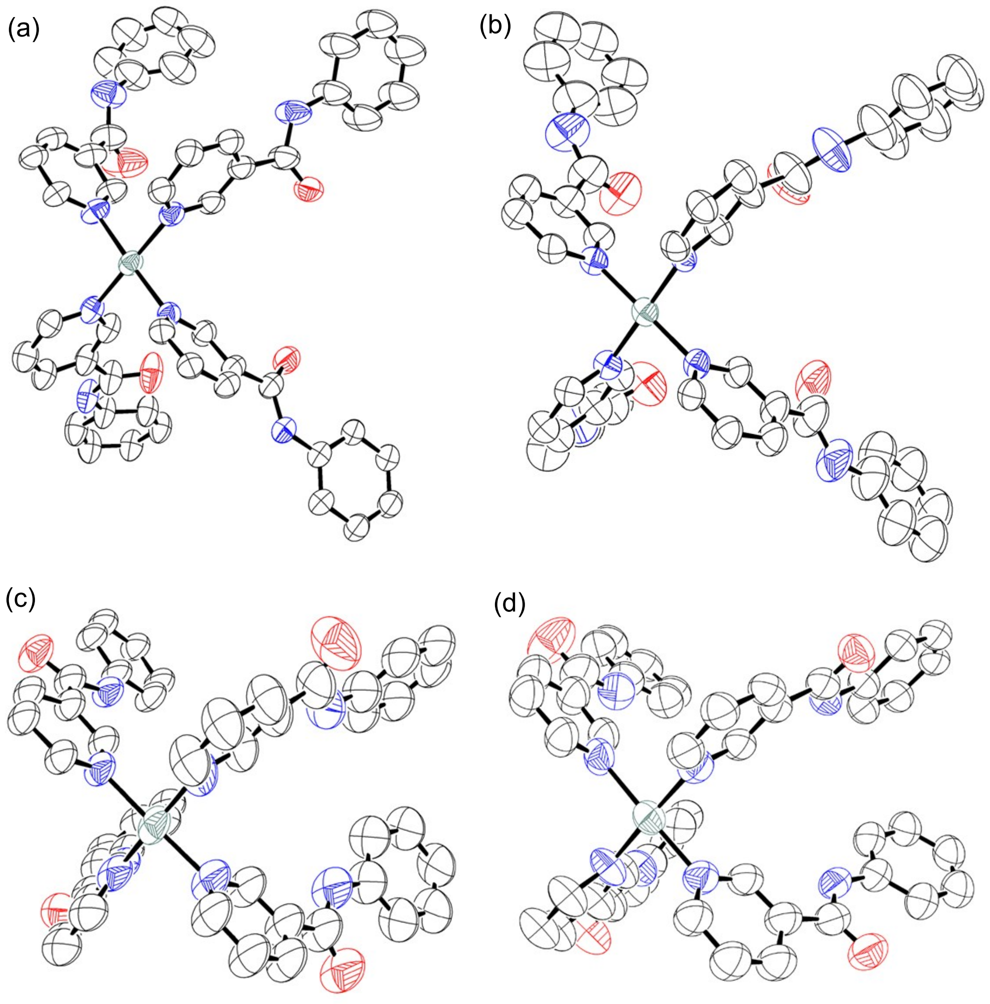

Fig. S18. ORTEP drawings showing Pd(II) geometries for **1**·$12NO_3$ (a), **1**·$12BF_4$ (b), **2**·$12C_8H_{17}OSO_3$ (c), and **2**·$12C_{12}H_{25}OSO_3$ (d), green: Pd^{2+}, black: C, red: O, blue, N, hydrogen atoms and anions were omitted for clarity.

.

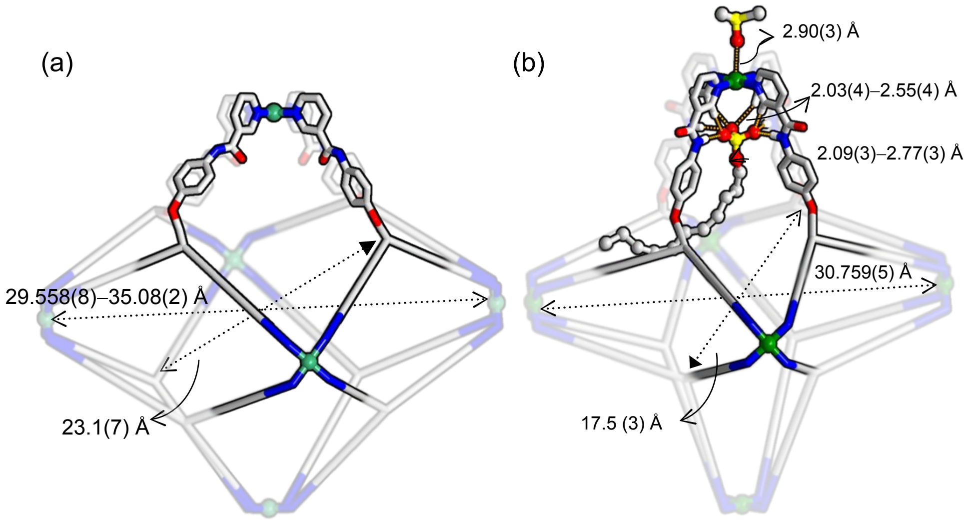

Fig. S19. The diameter (Pd···Pd distance) and molecular thicknesses for **1**·$12NO_3$ (a) and **2**·$12C_{12}H_{25}OSO_3$ (b) with highlighted intermolecular interactions.

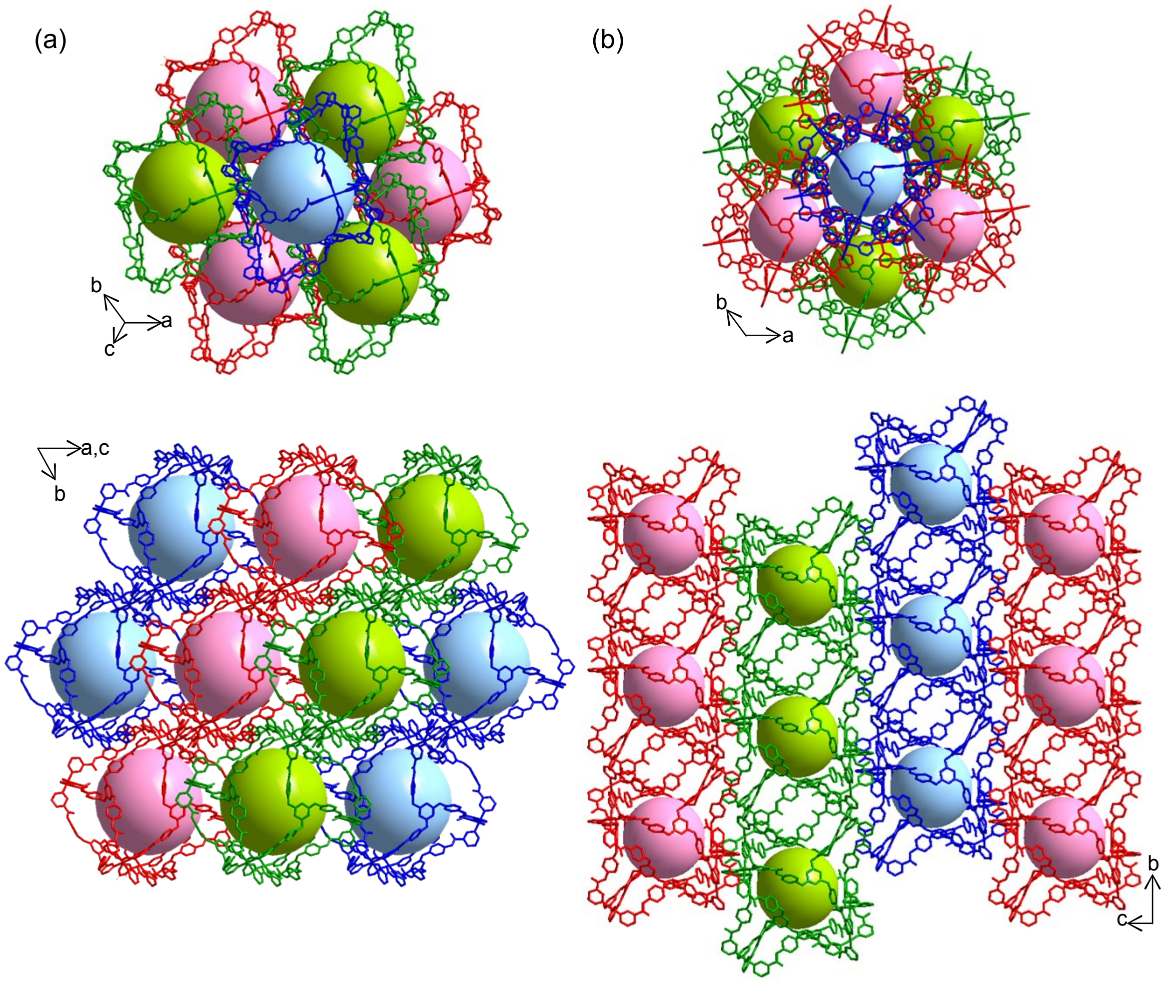

Fig. S20. Packing structures showing top (top) and side view (bottom) for **1**·12NO$_3$ (a) and **2**·12C$_{12}$H$_{25}$OSO$_3$ (b).

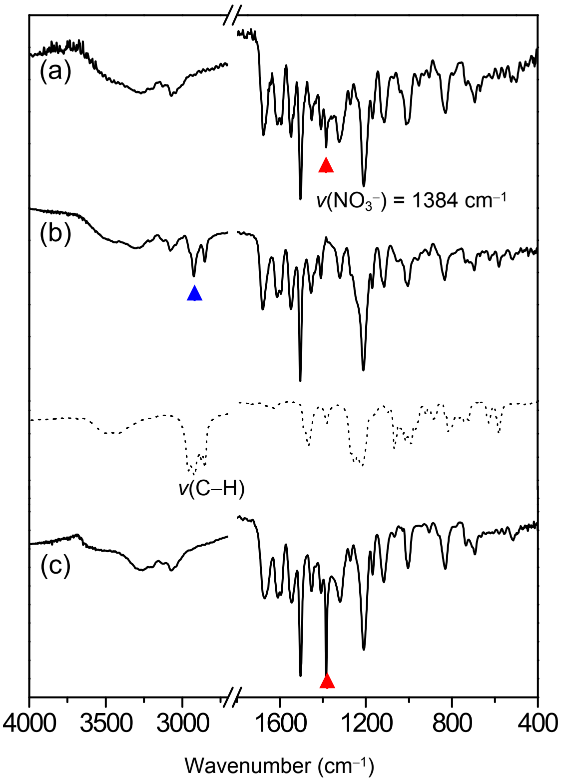

Fig. S21. IR spectra showing anion exchange experiment from NO_3^- to $C_{12}H_{25}OSO_3^-$. **1**·$12NO_3$ (a), sample after anion exchange (b), reversible anion exchange from $C_{12}H_{25}OSO_3^-$ to NO_3^- using an excess amount of NH_4NO_3 (100 equiv.) in the same solvent system at 40 °C (c), (black dotted line: $C_{12}H_{25}OSO_3^-NBu_4^+$).

Table S3. Contact angles for a drop of H_2O and 20% ethanol solution

Compounds	Contact Angle (°)			
	H_2O drop		H_2O/EtOH (4:1) drop	
	0 min	After 10 min	0 min	After 10 min
2·12$C_2H_5OSO_3$	102.20	80.54	98.30	78.78
2·12$C_8H_{17}OSO_3$	102.15	95.66	102.56	53.73
2·12$C_{10}H_{21}OSO_3$	102.80	98.17	101.13	46.57
2·12$C_{12}H_{25}OSO_3$	112.76	100.02	105.49	37.79
2·12$C_{14}H_{29}OSO_3$	114.87	100.8	99.94	35.84

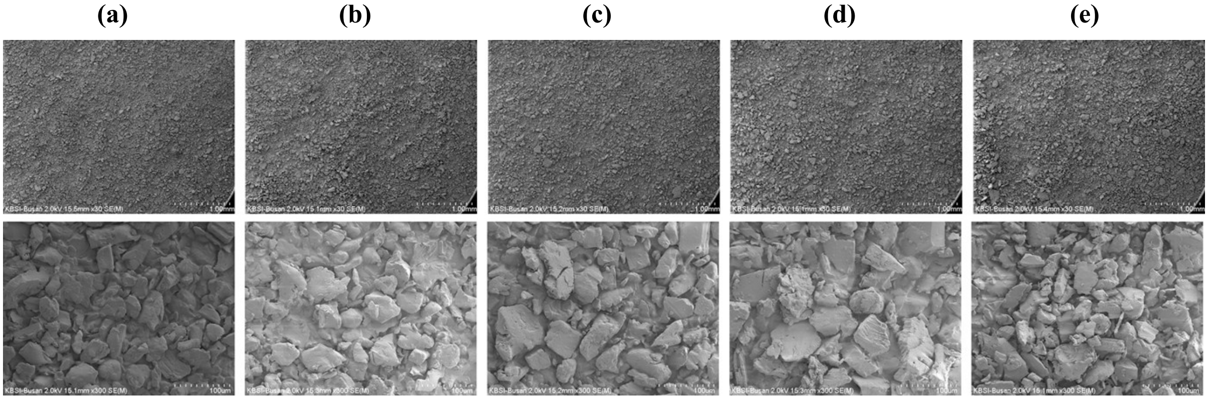

Fig. S22. SEM images of the surfaces **2**$\cdot 12C_2H_5OSO_3$ (a), **2**$\cdot 12C_8H_{17}OSO_3$ (b), **2**$\cdot 12C_{10}H_{21}OSO_3$ (c), **2**$\cdot 12C_{12}H_{25}OSO_3$ (d), and **2**$\cdot 12C_{14}H_{29}OSO_3$ (e).

References

1 J. W. Shin, K. Eom, D. Moon, *J. Synchrotron Rad.* 2016, **23**, 369-373.

2 Z. Otwinowski, W. Minor in *Methods in Enzymology*, *Vol. 276* (Eds.: C. W. Carter, Jr., R. M. Sweet), Academic Press, New York, 1997, part A, pp. 307.

3 G. M. Sheldrick, *Acta Cryst.* 2015, **A71**, 3–8.

4 G. M. Sheldrick, *Acta Cryst.* 2015, **C71**, 3–8.

5 A. L. Spek, *Acta Cryst.* 2009, **D65**, 148.

6 A. Thorn, B. Dittrich, G. M. Sheldrick, *Acta Cryst.* 2012, **A68**, 448.